





The Complex Nature of Magnetic Element Transport in the Quiet Sun: The Multiscaling Character

Fabio Giannattasio¹  and Giuseppe Consolini² 

¹ Istituto Nazionale di Geofisica e Vulcanologia, Via di Vigna Murata 605, I-00143 Roma, Italy; fabio.giannattasio@ingv.it

² INAF—Istituto di Astrofisica e Planetologia Spaziali, Via del Fosso del Cavaliere 100, I-00133 Roma, Italy
Received 2020 July 23; revised 2020 December 7; accepted 2020 December 24; published 2021 February 19

Abstract

In recent studies the dynamic properties of small-scale magnetic fields (magnetic elements [MEs]) in the quiet Sun were used to investigate peculiar features of turbulent convection and get insights on the characteristic spatial and temporal scales of evolution of magnetic fields, from granular to supergranular. The aim of this work is to extend previous studies and show that the displacement of MEs is compatible with a multiscaling behavior consistent with a Lévy motion. We tracked over 120,000 MEs in an unprecedented and uninterrupted set of high-resolution magnetograms acquired by the Hinode mission and targeted at quiet-Sun regions in the disk center, and we applied the multifractal diffusion entropy analysis to investigate the multiscaling character of ME transport in the quiet Sun. We found that the displacement of MEs in the quiet Sun exhibits a complex multiscaling behavior that cannot be described by a unique scaling law, as scaling exponents change with the scale considered. This result adds important physical constraints on turbulent convection and diffusion of MEs in the quiet Sun that future models need to account for.

Unified Astronomy Thesaurus concepts: Solar convective zone (1998); Solar magnetic fields (1503); Quiet sun (1322); Space weather (2037); Solar photosphere (1518)

1. Introduction

Understanding the dynamic properties of small-scale magnetic fields (hereafter magnetic elements [MEs]) in the solar photosphere is of uttermost importance in order to unveil the nature of turbulent convection and its capability to amplify and organize the magnetic fields, which are an effective vehicle for transferring energy to the upper atmospheric layers and start a chain of phenomena relevant to space weather (see, e.g., Alfvén 1947; Hart 1956; Parker 1957, 1988; Simon & Leighton 1964; November 1980; Roudier et al. 1998; Berrilli et al. 1999, 2002, 2004, 2005, 2013, 2014; Consolini et al. 1999; Del Moro 2004; Del Moro et al. 2004, 2015; Jefferies et al. 2006; Nesis et al. 2006; Viticchié et al. 2006; Centeno et al. 2007; De Pontieu et al. 2007; Tomczyk et al. 2007; de Wijn et al. 2008; Yelles Chaouche et al. 2011; Orozco Suárez et al. 2012; Giannattasio et al. 2013, 2014a, 2014b; Gošić et al. 2014, 2016; Sobotka et al. 2014; Stangalini et al. 2014, 2015, 2017; Stangalini 2014; Srivastava et al. 2017; Giannattasio et al. 2018).

The multiscaling properties of turbulent convection have long been investigated, but despite the efforts, a comprehensive model incorporating all the features that characterize turbulent convection at all scales and their coupling is still lacking. For this reason, alternative methods have been developed and improved to tackle the problem. By following this approach, in a recent paper Giannattasio et al. (2019) used the diffusion entropy analysis (DEA; Scafetta & Grigolini 2002) to detect the dynamical regime of MEs tracked in Hinode data. More in detail, they computed the probability distribution, $p(x, t)$, of MEs' displacement, x , and the associated Shannon entropy, $S(t)$. In a semi-log plot of entropy versus time, in the case of stationary and scale-invariant processes described by the probability density function (pdf) $p(x, t)$ and scaling exponent δ , $S(t)$ is a line with slope equal to δ . Thus, computing δ allows describing some dynamical properties of the MEs and,

consequently, of the velocity field that drags them along. Giannattasio et al. (2019) found that MEs in the quiet Sun undergo a common regime driven by turbulent convection and independent of the local environment. The emerging MEs' dynamics is ascribable to a Lévy walk, let us say a random walk with a heavy-tailed displacement distribution following a power law. This is a very important conclusion because such a dynamic behavior is known to characterize, for example, processes of turbulent diffusion, diffusion of Brownian particles in shear flows, diffusion of passive scalars in a turbulent flow, and turbulent regimes characterized by intermittency (see, e.g., Shlesinger et al. 1987, 1993; Hayot 1991; Zumofen et al. 1993; Malcai et al. 1999). For example, in intermittent regimes, energy dissipation is inhomogeneous and local both in space and in time, such that scaling features are not the same in the entire spatiotemporal domain but exhibit local properties described by the local (and not global) index δ . In this sense, the dynamics is multiscaling and/or multifractal.

Here we generalize the results in Giannattasio et al. (2019) and probe the possibility that the pdf's of displacement do not obey a monoscaling (fractal) law, characterized by a single scaling exponent, but conversely exhibit an anomalous scaling characterized by a multiscaling (multifractal) index. Again, here, we use an approach based on entropy (typically used for the study of complex systems) to point out and characterize the complex multiscaling nature of diffusion of MEs in the quiet Sun. This approach is an extension of the scaling analysis used in our previous paper (Giannattasio et al. 2019).

2. Observations and Data Analysis

2.1. The Data Set

We used the same seven different sets of magnetograms as in Giannattasio et al. (2019). They were acquired by the satellite Hinode (Kosugi et al. 2007; Tsuneta et al. 2008) in 2010 and targeted to different fields of view (FOVs) in the solar disk

center. These series have a common spatial resolution of $\sim 0.3''$ and an average noise level of ~ 4 G, which was computed as explained in detail in Gošić et al. (2014).

In Figure 1 we show the first magnetogram for each member of the set considered saturated between -100 and 100 G. Magnetograms were filtered out for 5-minute acoustic oscillations and segmented in order to identify MEs (Berrilli et al. 2005; Giannattasio et al. 2013), which were then tracked by using the algorithm described in Del Moro (2004) with the prescription that only MEs living for more than four subsequent frames were considered for further analysis. In particular, the segmentation of each magnetogram is obtained as follows: a starting threshold is defined as $B_T = 3\sigma$, i.e., three times the noise level. All the pixels with magnetic flux strength $> B_T$ are flagged as magnetic, while the rest are discarded. All the magnetic pixels that are clustered in features smaller than $A_{\max} = 50$ pixels (corresponding to an equivalent diameter of $\lesssim 1''$) are recognized as MEs and labeled. Instead, those clustered in features larger than A_{\max} are selected for the next iteration with the threshold raised by $\Delta B_T = 3\sigma$. The process is iterated until there are no more connected regions larger than A_{\max} in the magnetogram. The labeled MEs are then tracked forward in time starting from the first magnetogram in which they appear. To this aim, each ME present in the following magnetogram whose centroid is within a distance $\lesssim 3''$ from the original one is compared in shape by checking the distribution of magnetic pixels. The closest match, if any, is retained as the evolution of the original element. If the search in the next frame fails, it is extended to the next two frames; otherwise, it stops and the trajectory of the structure ends. All the features successfully tracked for more than four frames are used in the following analysis.

Table 1 summarizes the main characteristics of the data set used in this work, namely, the duration without interruption of each magnetogram set, its time cadence, the number of MEs tracked, and the lifetime of the longest-living MEs. As we can see, 120,461 MEs were tracked with lifetimes ranging from $\simeq 5$ minutes to $\simeq 17.1$ hr, thus spanning almost all temporal scales from granular to supergranular. Of course, the shortest possible lifetimes found are biased by the selection criteria used.

2.2. Multifractal Diffusion Entropy Analysis

We aimed at investigating the scaling properties of the time series consisting in the displacement of all MEs in the complete data set listed in Table 1. The displacement $x(t)$ of each ME is defined as the distance at time t from the position of its first appearance. For a stationary and scale-invariant time series the pdf of displacements scales as a power law

$$p(x, t) = t^{-\delta} G(xt^{-\delta}), \quad (1)$$

where G is a smooth function and δ is the scaling exponent that incorporates the dynamic properties of the system characterized by the pdf $p(x, t)$. For example, in the special case of a pure Brownian random walk process G is a Gaussian function and $\delta = 0.5$.

According to Scafetta & Grigolini (2002), it is possible to determine δ with high precision by computing the Shannon entropy $S(t)$ (see also Giannattasio et al. 2019, for application to solar MEs), defined as

$$S(t) = - \int_{-\infty}^{\infty} p(x, t) \ln[p(x, t)] dx. \quad (2)$$

For scale-invariant $p(x, t)$ satisfying Equation (1), Equation (2) gives

$$S(t) = \delta \ln(t) + A, \quad (3)$$

with

$$A = - \int_{-\infty}^{\infty} G(w) \ln[G(w)] dw, \quad w = xt^{-\delta}.$$

This means that $S(t)$ is a linear function of $\ln(t)$ with slope δ . Thus, the knowledge of $p(x, t)$ only allows evaluating $S(t)$ and the exponent δ from Equations (2) and (3), respectively. This method is called diffusion entropy analysis (DEA; Scafetta & Grigolini 2002).

A generalization of the Shannon entropy allows dealing with time series that do not strictly obey a *single* scaling behavior but show a higher degree of complexity. In fact, most of the real complex systems exhibit *anomalous* features, such as a multiple-scaling (*multiscaling* or *multifractal*) behavior that may be localized and dependent on the fluctuation amplitude (such as in the presence of intermittency). In this case, instead of a single scaling exponent δ , a spectrum of scaling exponents is necessary to fully portray the scaling behavior. This is accounted for by introducing the multifractal index q and the scaling exponent spectrum $\delta(q)$ instead of the monoscaling exponent δ . The stationary and scale-invariant condition in Equation (1) becomes

$$p(x, t) = t^{-\delta(q)} G(xt^{-\delta(q)}). \quad (4)$$

Despite their more complex nature, these multiscaling features reflect the physical properties of the system that generate them; thus, the correct characterization of these time series may give important information on the dynamic properties of the system. In our case, again, the turbulent photospheric convective motions in the quiet Sun represent the physical complex system under consideration, and the displacement of all the MEs in the data set can be considered as the time series for which we want to investigate the scaling properties. Starting from the Shannon entropy, Rényi defined a one-parameter family of entropies of order $q > 0$ (Rényi 1961) as

$$H_q(t) = \frac{1}{1-q} \ln \left[\int_{-\infty}^{\infty} p(x, t)^q dx \right], \quad q \neq 1. \quad (5)$$

The Rényi entropies represent a generalization of the Shannon entropy for any order q , and it can be easily verified that the Shannon entropy $S(t)$ is obtained under the limit

$$S(t) = \lim_{q \rightarrow 1} H_q(t).$$

It is important to note that the multifractal parameter q acts like a magnifying glass, allowing us to focus on extreme events of $p(x, t)$ for large values of q and on regular events, those in the bulk of the distribution, for small values of q . We will return to this point in the next section. By plugging Equation (4) into Equation (5) and changing the integration variable to $y = xt^{-\delta(q)}$, we obtain, similarly to Equation (3),

$$H_q(t) = \delta(q) \ln(t) + B, \quad (6)$$

where this time

$$B = \frac{1}{1-q} \int_{-\infty}^{\infty} G(y)^q dy, \quad y = xt^{-\delta(q)}. \quad (7)$$

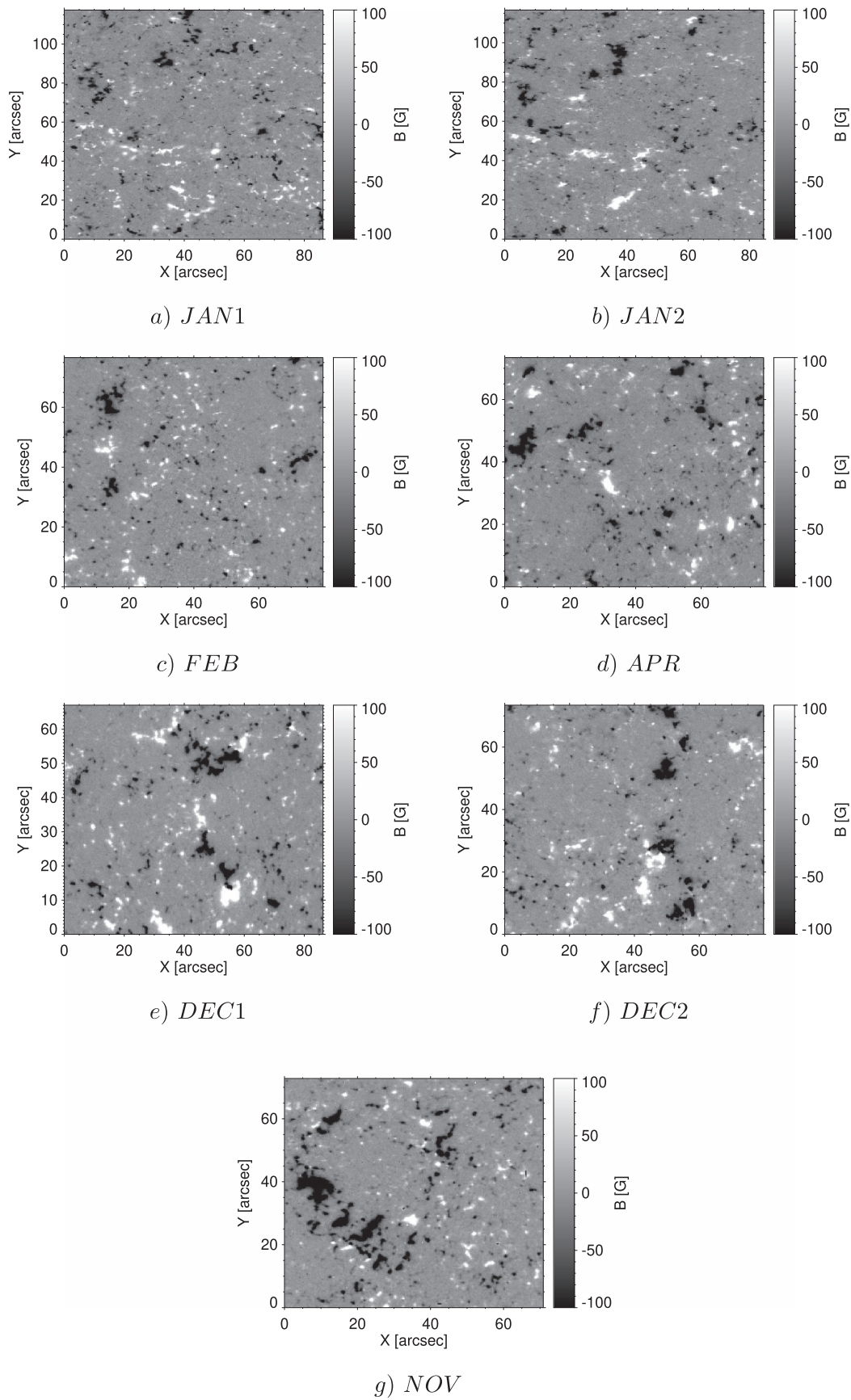


Figure 1. First magnetogram of the set for each of the seven FOVs representing the data set used in this work and listed in Table 1.

Table 1
Magnetogram Sets Employed

FOV	Duration (hr)	Time Cadence (s)	Num. of MEs	Maximum Lifetime (hr)
Jan 1	11.1	60	17,189	8.9
Jan 2	8.4	60	12,555	7.1
Feb	25.6	120	15,376	17.1
Apr	28.9	80	24,958	8.9
Dec 1	17.2	90	14,524	11.1
Dec 2	18.6	90	15,714	12.5
Nov	24.0	90	20,145	9.3

Again, $H_q(t)$ increases linearly with $\ln(t)$, the slope $\delta(q)$ being the spectrum of the scaling exponents for different values of the parameter q . Thus, starting from $p(x, t)$ only, it is possible to compute $H_q(t)$ using Equation (5), and subsequently $\delta(q)$ as the slope in a semi-log plot $H_q(t)$ versus $\ln(t)$ for different values of q . This procedure, called multifractal diffusion entropy analysis (MDEA), provides the spectrum of the scaling exponents in a system characterized by multiscaling diffusion processes.

3. Results and Discussion

The fundamental hypothesis beyond the investigation of turbulent convection in the quiet photosphere via the scaling analysis here performed is that the time series under investigation, $x(t)$, are stationary in some sense. This hypothesis is on the basis of both DEA and MDEA techniques. The stationarity of the time series was checked by using the Augmented Dickey–Fuller test (see, e.g., Fuller 1977; Said & Dickey 1984; Elliott et al. 1996). The procedure, which is well detailed in Giannattasio et al. (2019), basically models the displacement of MEs as an autoregressive process with a trend. According to this procedure, we found that the displacement time series of the MEs tracked, $x(t)$, is stationary with a very high confidence level (>99%).

In order to obtain further insights on the statistical properties of ME displacements and consequently constrain the dynamic properties of photospheric plasma in the quiet Sun, we analyzed the scaling of the time-dependent pdf's of displacements, $p(x, t)$. The pdf's obtained during the first 100 minutes are shown in the top panel of Figure 2, where the occurring time is encoded in colors from black to red. As we can see, $p(x, t)$ broadens with time, and the peak shifts, as expected, to gradually increasing displacements as MEs statistically move away from the starting point. For $t \lesssim 20$ minutes, the peak of $p(x, t)$ is at $\lesssim 0.5$ Mm. At longer times $p(x, t)$ becomes broader and broader owing to the diffusion rate, and the tails become more and more important, so as to affect substantially the displacement of MEs with respect to their initial position. When studying the scaling of diffusion phenomena, it is well known that in the case of scale-invariant pdf's exhibiting a self-similar behavior, Equation (1) should hold, and all pdf's should collapse onto a master curve P_δ . Data collapsing is, indeed, a very well known feature of self-similar processes, such as, for instance, Brownian and/or fractional Brownian motions. In such a situation, the observed distribution in space of a contaminant, which diffuses in time, can be collapsed into a single master curve in the case of a self-similar process. This is the signature for a simple monoscaling process. Conversely, when we deal with a multiscaling phenomenon, the data

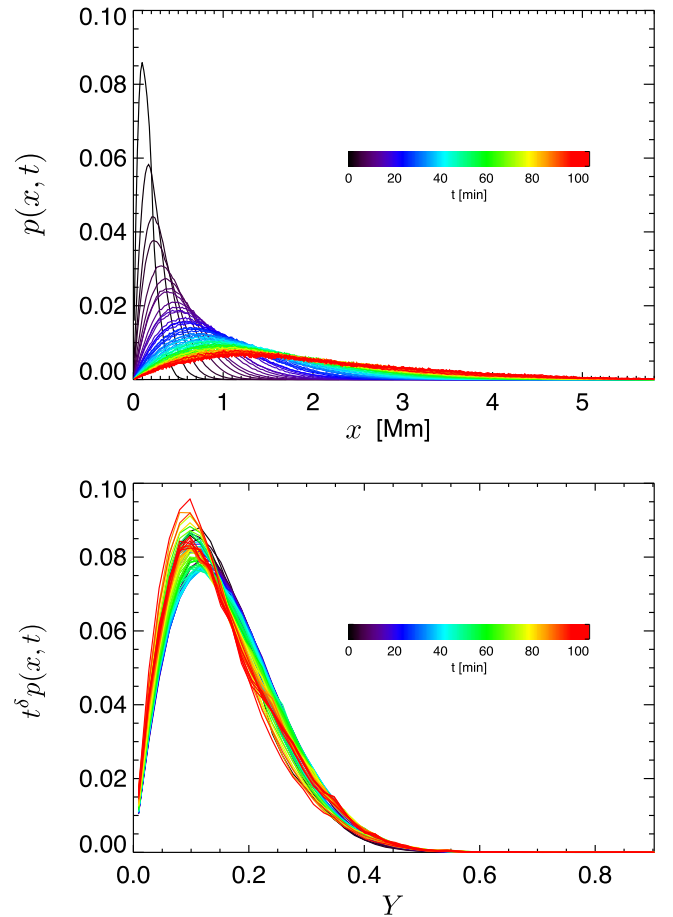


Figure 2. Top panel: pdf's of ME displacements, $p(x, t)$, as a function of time, which is encoded in colors from black to red. Bottom panel: collapsed pdf's via the transformation $Y = x/t^\delta$. See the text for more details. The color code is the same for both panels.

collapsing is generally missing. This is, for instance, the case of the dispersion of a passive scalar quantity in a turbulent environment.

The collapse of pdf's can be checked via the following transformation:

$$\begin{cases} x \rightarrow Y = x/t^\delta \\ p(x, t) \rightarrow t^\delta p(x, t) = P_\delta(x/t^\delta) \end{cases} \quad (8)$$

i.e., plotting the time-dependent rescaled pdf's $t^\delta p(x, t)$ versus Y . In their recent work, Giannattasio et al. (2019) showed, by using the DEA technique, that, independently of the FOV, MEs' displacement undergoes a common scaling that is very well fitted by a power law with slope $\zeta \simeq 0.62$. If this dynamic behavior were perfectly monoscaling, pdf's would collapse like in Equation (8) with the scaling factor t^ζ .

In the bottom panel of Figure 2 we show the results of the collapse obtained for $\delta = \zeta$, to be consistent with Giannattasio et al. (2019). As we can see, pdf's do not rigorously collapse onto a single P_δ , especially around the peak, which ranges between $Y = 0.10$ and $Y = 0.15$. This suggests two facts. First, the system has a higher degree of complexity rather than a “simple” universal monoscaling; this could be the evidence of a multiscaling behavior. Second, the emergence of a multiscaling character could be due to the occurrence of multiple phenomena, each being dominant in a specific range of scales.

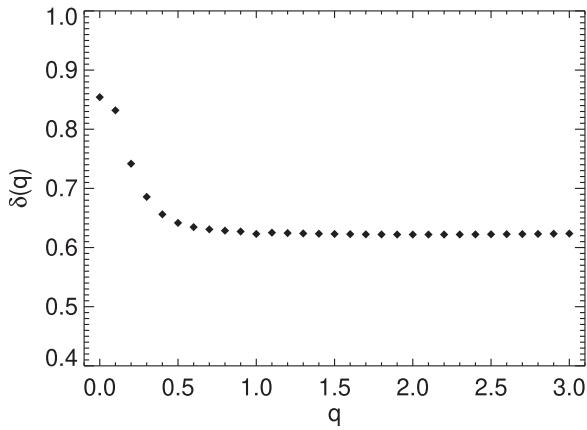


Figure 3. Scaling exponent spectra $\delta(q)$ as a function of the multifractal parameter q .

The emergence of multiscaling features may manifest in different scaling features (i.e., different scaling exponents) for the large and small increments as suggested in Chang & Wu (2008) and Consolini & de Michelis (2011), respectively. In other words, we have found an indication of the fact that the scaling of ME displacements cannot be rigorously described by a single scaling index, but a spectrum of indices is needed, each one representing the scaling behavior of displacements within a certain range of scales.

In order to get an estimate of the degree of complexity of the system, we adopted a multifractal approach and applied the MDEA technique. For any value of q in the range $0 \leq q \leq 3$ with steps 0.1 wide, we computed $H_q(t)$ according to Equation (5). The fit of this quantity versus the logarithm of time, following Equation (6), provided the scaling exponent (the slope of the fit) as a function of the parameter q , namely, the spectrum $\delta(q)$. The behavior of $\delta(q)$ is shown in Figure 3 (black diamonds). As we can see, the scaling exponents decrease from $\delta \simeq 0.85$ at $q=0$ down to $\delta \simeq 0.63$ at $q \simeq 0.6$, where δ reaches a plateau and remains almost constant up to $q=3$. The observed trend of the scaling exponents with q seems to indicate that these exponents follow a quasi-linear trend for $q \lesssim 0.5$ and then stabilize at larger q . This behavior is very similar to that observed in the case of a truncated Lévy process (Nakao 2000), whose multiscaling properties manifest in an at least *bi-fractal* feature, meaning that two different scalings emerge in the observed system. As clearly stated in Nakao (2000), a bi-fractal character of the observed scaling exponents represents the simplest case of a multiscaling behavior. In fact, in the case of a monofractal behavior, the scaling exponent $\delta(q)$ would scale linearly with q . Thus, the observed multiscaling character of ME motion can be the consequence of a broken self-similarity of the distribution of the displacements, as suggested in the paper by Nakao (2000).

To support this hypothesis, we have repeated the MDEA in the case of a smoothly truncated Lévy process with a characteristic Lévy index $\alpha = 0.4$ (Nakao 2000). Figure 4 shows the results of the corresponding scaling exponent spectrum, $\delta(q)$. The shape of the curve is very similar to that reported in Figure 3, supporting the hypothesis that the anomalous scaling may be a consequence of a quasi-bi-fractal nature of the ME motion.

The anomalous scaling shown here manifests as a change in the scaling properties of MEs' displacement distribution, from the bulk (highlighted by small values of q) to the tails

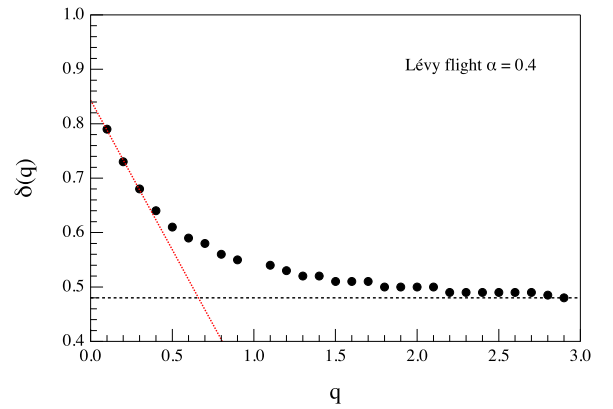


Figure 4. Scaling exponent spectra $\delta(q)$ as a function of q for a smoothly truncated Lévy process with a characteristic index $\alpha = 0.4$.

(highlighted by large values of q). The transition among the two regimes occurs at $q \simeq 0.6$, from a more *superdiffusive* regime (“superdiffusive” meaning that $\delta > 0.5$) for $q < 0.6$ to a more Brownian random walk regime ($\delta \simeq 0.6$) for $q > 0.6$.

The MDEA approach based on the Rényi entropy allowed us to show that the nature of the ME displacements is more complex than that described by a simple superdiffusive motion in a turbulent medium. This is clearly shown by the spectrum of scaling exponents $\delta(q)$. This spectrum indicates that the process driving the displacement of MEs, i.e., turbulent convection, has a multiscaling behavior. In particular, there is evidence of a bi-fractal behavior, similar to that studied, e.g., by Nakao (2000). Under this light, the varying parameter q is a magnifying glass with which to zoom in the various portions of the pdf's. In particular, for small values of q the Rényi entropy is dominated by the part of the pdf with more occurrences, i.e., nearby the peak. In this case $\delta(q)$ characterizes the scaling behavior of the *regular* events (i.e., the small-scale displacement of MEs), where particles (MEs, in our case) are statistically more clustered. On the contrary, the higher values of q zoom in the tails of the pdf, as in this case the regions of the distribution with fewer MEs dominate the Rényi entropy, and $\delta(q)$ describes the scaling behavior of the *extreme* events, where MEs are statistically sparse. To summarize, nearby the peak of the pdf (small q values), Rényi entropy highlights the regular paths according to which most of the MEs superdiffuse, while in the tails of the pdf (high q values) it highlights the extreme/rare events of ME displacement. Although according to Giannattasio et al. (2019) the response of MEs, as trackers of the underlying plasma flow, to turbulent convection is consistent with a Lévy walk, here we have clearly shown how such a dynamic behavior exhibits a more complex character. Indeed, the major novelty of our analysis is that ME displacement exhibits a multiscaling nature.

A question may arise: can imperfections of the tracking algorithm affect substantially the results obtained in this work? Of course, the displacement of MEs obtained via any tracking procedure may incorporate the predominant contribution of physical processes like turbulent convection together with the unavoidable contribution of nonphysical effects arising from the jittering of position of MEs. However, jittering, if present, affects all scales and adds a random contribution to displacements as it shortens or lengthens with the same probability the MEs' trajectories at any time. If this effect is dominant, we should observe a scaling exponent very close to 0.5 at all

scales. This does not happen, especially at small scales, indicating that jitter, if any, has a negligible effect with respect to the bulk (physical) dynamics. Moreover, even if present, jitter would not affect the main result of this work, namely, the multiscaling behavior and the transition among different dynamic regimes, as it would not generate any multiscaling regime compatible with a bi-fractal behavior.

4. Summary and Conclusions



Investigating the nature of the ME transport in the solar photospheres provides information on the properties of turbulent convection. Turbulence, in fact, is based on the processes occurring in the photosphere and involving all scales, from those under the resolution element to the global ones. Here, for the first time, we show the multiscaling nature of MEs' displacement and, thus, of the underlying plasma velocity field, by using a technique based on entropy. With this technique, called MDEA, we pointed out, as a result, that the scaling properties of the system as a whole cannot be described by a single value of the scaling index. In particular, we characterized the multiscale behavior of the pdf of displacements by computing the one-parameter spectrum of scaling exponents, $\delta(q)$. It is still not clear what are the mechanisms generating such a turbulent behavior, but for sure we can exclude classical models of turbulent cascade, like that of Kolmogorov. Specifically, we extended the results in Giannattasio et al. (2019), who discovered that turbulent diffusion in the solar photosphere is consistent with a Lévy walk, pointing out an even more complex behavior: small scales, which sample the bulk of the pdf of displacements, show scaling properties different from those at large scales, which sample the extreme displacements of the pdf. This implies a different dynamics for bulk motion on smaller scales and longer walks involving larger scales. The smooth transition among these regimes occurs at $q \simeq 0.6$. To conclude, the results presented in this work for ME displacement on scales from granular to supergranular (Figure 3) show that the transport of MEs is governed by a complex dynamics characterized by a multiscaling nature and consistent with a bi-fractal behavior. We believe that these findings are important in shedding light on the nature of turbulent convection and the properties of velocity field and magnetic field organization in the quiet photosphere.

As a future perspective, it would be interesting to investigate the scaling features of displacement of MEs belonging to internetwork (IN) and network (NE) regions by applying DEA and MDEA techniques described in Giannattasio et al. (2019) and in this work, respectively. In fact, it is well known that both types of magnetic features may have different dynamics owing to their different origins, sizes, structures, locations, flux contents, magnetic field strengths, etc., as also pointed out by, e.g., Giannattasio et al. (2014b, 2018). This will provide an indication of whether or not the multiscaling character emerging in the quiet Sun is due to different behaviors observed in IN and NE regions or is a universal property common to all MEs in the quiet Sun.

This work is supported by Italian MIUR-PRIN grant 2017APKP7T on Circumterrestrial Environment: Impact of Sun-Earth Interaction. This paper is based on data acquired in the framework of the Hinode Operation Plan 151 entitled “Flux

replacement in the network and internetwork.” Hinode is a Japanese mission developed and launched by ISAS/JAXA, collaborating with NAOJ as a domestic partner, NASA and STFC (UK) as international partners. Scientific operation of the Hinode mission is conducted by the Hinode science team organized at ISAS/JAXA. This team mainly consists of scientists from institutes in the partner countries. Support for the post-launch operation is provided by JAXA and NAOJ (Japan), STFC (U.K.), NASA, ESA, and NSC (Norway).

ORCID iDs

Fabio Giannattasio  <https://orcid.org/0000-0002-9691-8910>
Giuseppe Consolini  <https://orcid.org/0000-0002-3403-647X>

References

- Alfvén, H. 1947, *MNRAS*, 107, 211
Berrilli, F., Consolini, G., Pietropaolo, E., et al. 2002, *A&A*, 381, 253
Berrilli, F., Del Moro, D., Consolini, G., et al. 2004, *SoPh*, 221, 33
Berrilli, F., del Moro, D., Florio, A., & Santillo, L. 2005, *SoPh*, 228, 81
Berrilli, F., Florio, A., Consolini, G., et al. 1999, *A&A*, 344, L29
Berrilli, F., Scardigli, S., & Del Moro, D. 2014, *A&A*, 568, A102
Berrilli, F., Scardigli, S., & Giordano, S. 2013, *SoPh*, 282, 379
Centeno, R., Socas-Navarro, H., Lites, B., et al. 2007, *ApJL*, 666, L137
Chang, T., & Wu, C.-C. 2008, *PhRvE*, 77, 045401
Consolini, G., Carbone, V., Berrilli, F., et al. 1999, *A&A*, 344, L33
Consolini, G., & de Michelis, P. 2011, *NPGeo*, 18, 277
De Pontieu, B., McIntosh, S. W., Carlsson, M., et al. 2007, *Sci*, 318, 1574
de Wijn, A. G., Lites, B. W., Berger, T. E., et al. 2008, *ApJ*, 684, 1469
Del Moro, D. 2004, *A&A*, 428, 1007
Del Moro, D., Berrilli, F., Duvall, T. L. J., & Kosovichev, A. G. 2004, *SoPh*, 221, 23
Del Moro, D., Giannattasio, F., Berrilli, F., et al. 2015, *A&A*, 576, A47
Elliott, G., Rothenberg, T. J., & Stock, J. H. 1996, *Econometrica*, 64, 813
Fuller, W. A. 1977, *J. Roy. Statist. Soc. Ser. A*, 140, 379
Giannattasio, F., Berrilli, F., Biferale, L., et al. 2014a, *A&A*, 569, A121
Giannattasio, F., Berrilli, F., Consolini, G., et al. 2018, *A&A*, 611, A56
Giannattasio, F., Consolini, G., Berrilli, F., & Del Moro, D. 2019, *ApJ*, 878, 33
Giannattasio, F., Del Moro, D., Berrilli, F., et al. 2013, *ApJL*, 770, L36
Giannattasio, F., Stangalini, M., Berrilli, F., Del Moro, D., & Bellot Rubio, L. 2014b, *ApJ*, 788, 137
Gošić, M., Bellot Rubio, L. R., del Toro Iniesta, J. C., Orozco Suárez, D., & Katsukawa, Y. 2016, *ApJ*, 820, 35
Gošić, M., Bellot Rubio, L. R., Orozco Suárez, D., Katsukawa, Y., & del Toro Iniesta, J. C. 2014, *ApJ*, 797, 49
Hart, A. B. 1956, *MNRAS*, 116, 38
Hayot, F. 1991, *PhRvA*, 43, 806
Jefferies, S. M., McIntosh, S. W., Armstrong, J. D., et al. 2006, *ApJL*, 648, L151
Kosugi, T., Matsuzaki, K., Sakao, T., et al. 2007, *SoPh*, 243, 3
Malcai, O., Biham, O., & Solomon, S. 1999, *PhRvE*, 60, 1299
Nakao, H. 2000, *PhLA*, 266, 282
Nesis, A., Hammer, R., Roth, M., & Schleicher, H. 2006, *A&A*, 451, 1081
November, L. J. 1980, PhD thesis, Colorado Univ, Boulder
Orozco Suárez, D., Katsukawa, Y., & Bellot Rubio, L. R. 2012, *ApJL*, 758, L38
Parker, E. N. 1957, *JGR*, 62, 509
Parker, E. N. 1988, *ApJ*, 330, 474
Rényi, A. 1961, in *Proc. 4th Berkeley Symp. Mathematical Statistics and Probability 1*, ed. J. Neyman (Berkeley: Univ. California Press), 547
Roudier, T., Malherbe, J. M., Vigneanu, J., & Pfeiffer, B. 1998, *A&A*, 330, 1136
Said, S. E., & Dickey, D. A. 1984, *Biometrika*, 71, 599
Scafetta, N., & Grigolini, P. 2002, *PhRvE*, 66, 036130
Shlesinger, M. F., West, B. J., & Klafter, J. 1987, *PhRvL*, 58, 1100
Shlesinger, M. F., Zaslavsky, G. M., & Klafter, J. 1993, *Natur*, 363, 31

- Simon, G. W., & Leighton, R. B. 1964, *ApJ*, 140, 1120
- Sobotka, M., Švanda, M., Jurčák, J., et al. 2014, *CEAB*, 38, 53
- Srivastava, A. K., Shetye, J., Murawski, K., et al. 2017, *NatSR*, 7, 43147
- Stangalini, M. 2014, *A&A*, 561, L6
- Stangalini, M., Consolini, G., Berrilli, F., De Michelis, P., & Tozzi, R. 2014, *A&A*, 569, A102
- Stangalini, M., Giannattasio, F., Erdélyi, R., et al. 2017, *ApJ*, 840, 19
- Stangalini, M., Giannattasio, F., & Jafarzadeh, S. 2015, *A&A*, 577, A17
- Tomczyk, S., McIntosh, S. W., Keil, S. L., et al. 2007, *Sci*, 317, 1192
- Tsuneta, S., Ichimoto, K., Katsukawa, Y., et al. 2008, *SoPh*, 249, 167
- Viticchié, B., Del Moro, D., & Berrilli, F. 2006, *ApJ*, 652, 1734
- Yelles Chaouche, L., Moreno-Insertis, F., Martínez Pillet, V., et al. 2011, *ApJL*, 727, L30
- Zumofen, G., Klafter, J., & Blumen, A. 1993, *PhRvE*, 47, 2183